European Journal of Pharmaceutical Sciences 212 (2025) 107152

Contents lists available at ScienceDirect

European Journal of Pharmaceutical Sciences

journal homepage: www.elsevier.com/locate/ejps

Guiding excipient selection for physically stable amorphous solid dispersions: A combined in-vitro in-silico approach

Egis Zeneli [a,b,c], Hugo Bohets [c], Frédéric Ngono Mebenga [c], René Holm [d], Christophe Tistaert [c], Martin Kuentz [b,*]

[a] University of Basel, Department of Pharmaceutical Sciences, Klingelbergstrasse 50, Basel 4056, Switzerland
[b] University of Applied Sciences and Arts Northwestern Switzerland, Institute of Pharma Technology Hofackerstr. 30, CH-4132 Muttenz, Switzerland
[c] Janssen Pharmaceutica, Turnhoutseweg 30, Beerse 2340, Belgium
[d] University of Southern Denmark, Department of Physics, Chemistry and Pharmacy Campusvej 55, Odense 5230, Denmark

ARTICLE INFO

Keywords:
Amorphous solid dispersion
Physical stability
High-throughput screening
COSMO-RS

ABSTRACT

Fast screening of amorphous solid dispersions (ASDs) is a need in the pharmaceutical industry. To support this, several emerging technologies have been developed ranging from in-silico prediction to miniaturized high-throughput experimentation. However, a notable challenge lies in the absence of comparative data. In the present work, a combination of a miniaturized screening of ASDs with calculation of activity coefficients using the conductor like screening model for real solvents (COSMO-RS) was proposed. First, the physical stability of ASDs comprising drugs of different glass forming ability (GFA) each with ten pharmaceutically relevant polymers was evaluated under accelerated stress conditions at two drug:polymer ratios. The miniaturized high-throughput screening method was based on the instability onset time that was monitored by polarized light microscopy (PLM). Furthermore, COSMO-RS was used to assess the interaction strength between the drugs and polymers by calculating activity coefficients, which was combined with estimations of the wet glass transition temperature (T_g), to account for molecular mobility. The computational calculations showed an overall alignment of 87 % with the instability of the ASDs observed experimentally for comparable drug:polymer ratios and humidity conditions. This positive result supports the current understanding of stable ASD formulation where at given ambient conditions, a low molecular mobility as well as the strength of interaction between drug and polymer has a main impact on the physical stability of ASDs. The current results are further encouraging to implement such a combined in-vitro/high-throughput (HTS) and in-silico strategy in early industrial screening of ASDs.

1. Introduction

An increasing number of new active pharmaceutical ingredients (APIs) in the pharmaceutical pipeline exhibit poor water solubility, affecting absorption and ultimately bioavailability of the drug (Peter van Hoogevest et al., 2011). Absorption of a drug via the oral route is primarily dependent on three aspects; i) solubility, ii) dissolution rate, and iii) intestinal permeability, which can all lead to inadequate absorption if the extent of these parameters is not sufficient relative to the API dose. Preparation of amorphous solid dispersions (ASDs) provides a promising tool to obtain an improved apparent solubility and dissolution rate (Zhang et al., 2019, Wolbert et al., 2022, Rumondor et al., 2009). ASDs are composed of drug, in the amorphous form, mixed in a polymeric carrier, which generally improves aqueous kinetic solubility relative to the crystalline form of the compound due to a higher Gibbs free energy (Kapourani et al., 2020). Furthermore, the presence of polymeric carriers can improve wetting of the API, resulting in improved dissolution and possibly enhanced drug absorption (Lehmkemper et al., 2017, Newman and Zografi, 2023). From manufacturing to administration, there are multiple stages where the API of an ASD crystallize. These include; i) non-homogeneous blending of the ASD components during manufacture, ii) instability during shelf life, and iii) potential precipitation of the API in vivo following oral administration (Ricarte et al., 2019). Through selection of a suitable polymer, one should achieve a desired release of the API from the formulation, avoid/delay precipitation in vivo, and improve shelf life (Taylor and Zhang, 2016, Que et al., 2021). The polymeric carrier has therefore a three-faceted function. Firstly, and secondly, it can affect the rate and extent of drug

* Corresponding author.
E-mail addresses: reho@sdu.dk (R. Holm), CTISTAER@its.jnj.com (C. Tistaert), martin.kuentz@fhnw.ch (M. Kuentz).

https://doi.org/10.1016/j.ejps.2025.107152
Received 28 February 2025; Received in revised form 7 May 2025; Accepted 28 May 2025
Available online 6 June 2025

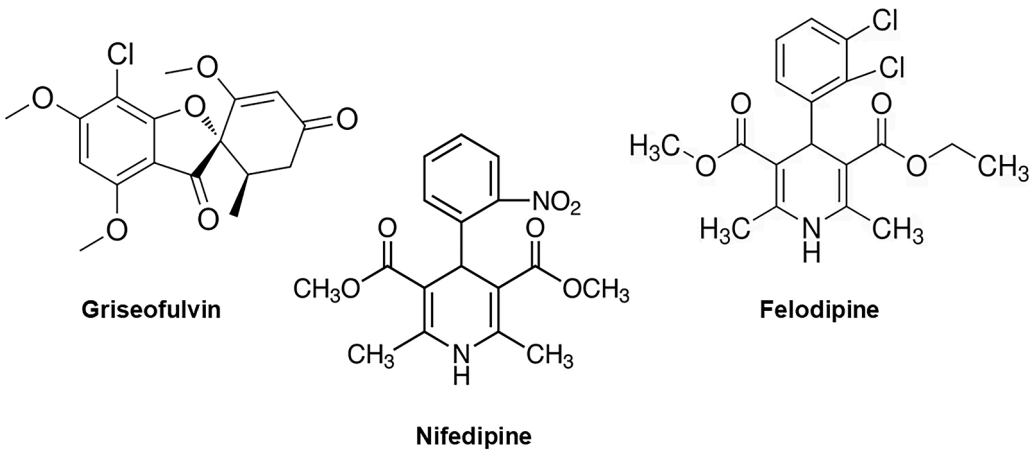

Fig. 1. Chemical structures of the model compounds.

release behavior from an ASD as the API must be released within the gastrointestinal transit time to achieve efficient oral absorption (Dukeck et al., 2013). Thirdly, selection of an appropriate carrier is key for achieving the desired physical stability over the entire shelf-life of the drug product, which is influenced by three main components: thermodynamic, kinetic, and environmental parameters (Baird and Taylor, 2012). For ASDs, the amount of drug in the polymeric carrier typically exceeds the solubility in the polymer so it can result in phase separation and recrystallization of the API (Tian et al., 2020, Tian et al., 2016, Ilevbare and Taylor, 2013). For stability reasons it is, hence, crucial to consider the glass transition temperature when selecting a polymeric carrier (T_g). When the temperature is kept clearly below the T_g, the ASD is in a glassy state and to some extent kinetically stabilized, as especially the molecular α-relaxations are immobilized (Kothari et al., 2014). Contrary, when the storage stability is above the glass transition temperature, the molecules within the ASD are in the supercooled liquid state and therefore have a higher degree of mobility, leading to a higher instability increasing the chance/risk of recrystallization (Li et al., 2015, Kapourani et al., 2020, Kothari et al., 2014). As a general guideline, many studies suggest a storage temperature below T_g - 50 K to ensure good physical stability of the ASD (Baird and Taylor, 2012, Taylor and Zhang, 2016). Therefore, using a polymer with a high glass transition temperature can result in a reduction of the overall molecular mobility and consequently increased physical stability (Hiew et al., 2022). With respect to such a kinetic stabilization, Baird and Taylor reported a positive correlation between molecular mobility of ASDs and the degree of recrystallization (Baird et al., 2010). Another important parameter to be considered is drug- polymer compatibility and hence intermolecular interactions between the two. Favorable intermolecular interactions translate into good miscibility to avoid or inhibit a phase separation that would eventually lead to drug recrystallization (Taylor, 2009). Finally, importance should be given to environmental factors such as relative humidity (RH) and temperature, which can indirectly affect the thermodynamic and kinetic properties of the ASD (Lin et al., 2018). For example, an increase in temperature can result in increased molecular mobility within the ASD and destabilize the system (Xie and Taylor, 2017). The presence of water on the other hand, has a plasticizing effect by breaking the intermolecular interactions and accelerating processes such as nucleation and crystal growth (Tian et al., 2016, Lin et al., 2018). Recrystallization of the API in this instance would affect not only physical stability, but also solubility and the biopharmaceutical product performance (Taylor and Zhang, 2016, Baird and Taylor, 2012). Thus, many factors can influence physical stability of an ASD making the screening for suitable excipients challenging and it is therefore currently still a trial-and-error process (Dukeck et al., 2013, Newman and Zografi, 2023). Despite reported applications of high-throughput methods in the pharmaceutical field to accelerate early formulation development, adequate excipient selection remains a lengthy and costly process, which is further limited by little API availability, particularly at the early discovery and development stages (Wyttenbach et al., 2007, Wyttenbach et al., 2013). This highlights the need for non-empirical methods, such as computational models, to help guide excipient selection. Recently, computational methods have been applied with good success to the drug development field (Kuentz et al., 2021). For example, molecular dynamics (MD) simulations have been used to assess drug-polymer interactions, while also the combined quantum-chemical and thermodynamic approach of the conductor-like screening model for real solvents, COSMO-RS, has been reported as promising regarding formulation development (Kuentz et al., 2021, Aulifa et al., 2024, Xiang and Anderson, 2013). COSMO-RS has been applied within the pharmaceutical industry for drug property prediction and first attempts have been made to support oral and parenteral formulation development (Loschen and Klamt, 2015, Aulifa et al., 2024). In a recent study, Price and co-workers applied COSMO-RS successfully for the selection of precipitation inhibitors (Price et al., 2019). Furthermore, COSMO-RS has been used to predict API solubility in several media (Loschen and Klamt, 2015). Very recently, Antolovic and coworkers used the COSMO-SAC model to predict API-polymer compatibility (Antolovic et al., 2024). The investigation by Antolovic et al. included both solubility and miscibility aspects of different APIs with a series of polymers and it was reported that overall, the estimations were reasonable although individual predictions clearly deviated from experimental results (Antolovic et al., 2024). Moreover, from a qualitative perspective, the model correctly ranked polymers based on their compatibility with the API. In the current work the main goal was to evaluate COSMO-RS as supportive tool, to experimental high-throughput screening methods, to guide excipient selection at the early stages of ASD development. Firstly, a miniaturized high-throughput screening method was used to prepare ASDs of griseofulvin, nifedipine and felodipine in the presence of ten pharmaceutically relevant polymers, at two ratios. Further, the physical stability of the obtained ASDs was investigated under accelerated stress conditions over a three-month period. The onset of instability of the ASDs was related to the interaction strength between API and polymer, by means of activity coefficients calculated by COSMO-RS, to compare in-silico results and in-vitro experiments. Moreover, considering the importance of molecular mobility, the glass transition temperature (T_g) of the ASDs was estimated using the Gordon-Taylor equation, which allowed for a more educated comparison of ASDs and predicted activity coefficients within a given mobility domain.

2. Materials and methods

Nifedipine was purchased from Thermo Fisher Scientific (Dreieich, Germany). Felodipine was obtained from TCI Europe (Eschborn,

Table 1
Estimated glass transition temperatures (T_g) of the neat active pharmaceutical ingredients (APIs) and polymers and densities used for the Gordon-Taylor equation.

	Component	Density (g/cm^3)	T_g (°C)	T_g References
API	Griseofulvin (GFA I)	1200	89	(Baird et al., 2010)
	Nifedipine (GFA II)	1200	45	(Baird et al., 2010)
	Felodipine (GFA III)	1200	45	(Baird et al., 2010)
Polymer	PVP K30	1712.6	162.5	(Asgreen et al., 2020)
	PVP VA 64	1455.0	101	(BASF, 2022)
	HPMC E5	1327.8	154	(Honary and Orafai, 2002)
	HPMC AS LG	1280.1	119	(Butreddy, 2022)
	HPMC AS MG	1306.7	120	(Butreddy, 2022)
	HPMC AS HG	1265.5	122	(Butreddy, 2022)
	Eudragit E100	804.6	48	(Patra et al., 2017)
	Eudragit L100	1150.1	195	(Moustafine et al., 2006)
	Eudragit L100 55	1190.0	111	(Moustafine et al., 2006)
	Soluplus	1187.7	70	(BASF, 2024)

Germany) and griseofulvin was purchased from Sigma-Aldrich (Darmstadt, Germany). HPMC AS grades LG, MG and HG were purchased from Shin Etsu AQOAT (Chigasaki, Japan), Eudragit grades E100, L100 and L100 55 were obtained from Evonik (Essen, Germany), Soluplus, PVP K30 and PVP VA 64 were purchased from BASF (Ludwigshafen, Germany) and HPMC E5 was obtained from VWR (Leuven, Belgium).

2.1. Preparation of amorphous solid dispersions

ASDs of griseofulvin, nifedipine and felodipine were casted to films in combination with ten pharmaceutically relevant polymers. The chemical structure of the model APIs can be seen in Fig. 1. Drug stock and polymer stock solutions were prepared separately in dichloromethane:methanol solvent mixture (1:1). Subsequently, the polymer and API stock were used to prepare API:polymer master mixes in a 1:2 and 1:3 (w/w) ratio using the Hamilton Microlab STAR liquid handling robot (Gräfelfing, Germany). Nifedipine is a light-sensitive compound and was therefore protected whenever possible. 100 µg films were casted in 1 mL flat bottom glass vials (LOADEF 96- tray) from Screening Devices, followed by quick solvent evaporation at 70 °C under vacuum for one hour in a Heraeus Vacutherm oven from Thermo Scientific (Dreieich, Germany). All samples were casted in triplicates, including neat API and neat polymer controls.

2.2. Accelerated stability studies

The casted ASD films were stored under the following three stress conditions: (a) 40 °C and 75 %RH, (b) 50 °C and 75 %RH, and (c) 50 °C and 30 %RH, to assess both the impact of temperature and humidity over a three-month period. Samples were stored in WKL temperature and humidity- controlled chambers from Weiss (Buchen, Germany). All samples were stored in darkness, with minimal light exposure during handling to mitigate relevant chemical degradation, which could otherwise lead to physical instability. After defined intervals of 0, 2, 7, 21, 42, 63, and 84 days, the casted ASDs were investigated for recrystallization by a custom-made Polarized Light Miscroscopy (PLM) Vision Station from Vision Engineering (Surrey, UK). Photographs were taken using a GV-5890CP-C-HQ Rev. 2.2 camera from Imaging Development Systems (Obersulm, Germany) and a Vision Recorder by Exmore (Beerse, Belgium). Images were assessed visually for onset and growth of instability/crystallization. However, a quantification of crystallinity or further instrumental physical bulk analytics was considered beyond scope of the present work on early ASD screening. Thus, an initial categorization into fully amorphous, instability onset time (moderate PLM signal) and high PLM signal is provided. The timepoint at which birefringence expanded compared to the instability onset time was categorized as high PLM signal observed.

2.3. Estimation of the Gordon Taylor Glass transition temperature

The wet glass transition temperature of the ASD systems was calculated to estimate the mobility domain for each ASD. For this purpose, the Gordon-Taylor equation was used, as shown below in equation .1;

$$Tg = \frac{\Sigma_i K_i w_i T_{g,i}}{\Sigma_i K_i w_i} \quad (1)$$

where w_i are the wt % components in the wet system (API, polymer and water) and $T_{g,i}$ are the respective glass transition temperatures, expressed in Kelvin

T_g values available in the literature were used for the APIs and studied polymers and can be found in Table 1.

K_i parameter was calculated from the densities (ρ) of the pure components and pure glass transition temperatures, using equation 2. The parameter i is representative of the ASD components, API, polymer or water.

$$K_i = \frac{\rho_{API} T_{g,API}}{\rho_i T_{g,i}} \quad (2)$$

Water sorption measurements at ambient temperature were used in the calculation, assuming the overall ranking of polymers would not change at the higher tested temperatures. The amorphous density of the APIs was assumed to be 1.2 which was about 90-95 % of the density of crystalline APIs, generally falling between 1.4 and 1.6.

2.4. Estimation of the water uptake of the ASDs

To mimic the experimentally tested physical stability conditions, the water uptake of the ASDs was estimated at 30 %RH and 75 %RH at 25 °C. Although the ASDs were incubated at 40 °C and 50 °C, it was assumed that the water uptake as qualitative ranking would not change relative to the ranking obtained at 25 °C. Internal dynamic vapor sorption (DVS) values were measured with a DVS Intrinsic PLUS from Surface measurement Systems (London, UK), which for the tested polymers can be found in Table S1 in the supplementary materials. No DVS measurements were performed for the crystalline poorly water-soluble APIs (given their low hygroscopicity), instead the water sorption behavior was estimated to be 0.6 at 30 %RH and 1.7 for measurements at 75 %RH. These values were used to estimate the water uptake of the ASDs at an API:polymer ratio of 1:2 and 1:3 (w/w). The results obtained can be seen in Table S2 in the supplementary materials.

2.5. COSMO-RS modeling

The Conductor Like Screening Model for Real Solvents (COSMO-RS) has its foundations in the conductor-like-screening model (COSMO) and has been previously described in the literature (Klamt and Eckert, 2000, Klamt, 2011). The theoretical approach is related to the dielectric

Table 2
Onset of instability in days for the studied amorphous solid dispersions, ASDs at the investigated stress conditions over a three-month period. Only the unstable combinations are included.

Polymer	Griseofulvin					
	1:2 (w/w) API:Polymer			1:3 (w/w) API:Polymer		
	40°C/75RH	50°C/75RH	50°C/30RH	40°C/75RH	50°C/75RH	50°C/30RH
Neat API	2	2	2	2	2	2
PVP K30	2	2	>84	2	2	>84
PVP VA 64	2	2	>84	7	7	>84
Soluplus	7	2	42	7	2	84
HPMC E5	2	63	>84	2	84	>84
HPMC AS LG	42	7	>84	63	21	>84
HPMC AS MG	21	21	>84	21	42	>84
HPMC AS HG	>84	21	>84	>84	21	>84
Polymer	**Nifedipine**					
	1:2 (w/w) API:Polymer			1:3 (w/w) API:Polymer		
	40°C/75RH	50°C/75RH	50°C/30RH	40°C/75RH	50°C/75RH	50°C/30RH
Neat API	2	2	2	2	2	2
PVP K30	42	84	>84	84	>84	>84
HPMC E5	63	84	>84	63	84	>84
Eudragit L100 55	63	42	>84	63	42	>84
Polymer	**Felodipine**					
	1:2 (w/w) API:Polymer			1:3 (w/w) API:Polymer		
	40°C/75RH	50°C/75RH	50°C/30RH	40°C/75RH	50°C/75RH	50°C/30RH
Neat API	21	21	21	21	21	21

continuum solvation models (PCM), but with a few advantages. For example, contrary to the classic PCM models, it can distinguish between two solvents with identical dielectric constants. Furthermore, it enables consistent thermodynamic behavior calculations of mixture properties across varying temperatures, making it applicable to a variety of fields that were previously not accessible to continuum models (Diedenhofen and Klamt, 2010, Klamt and Eckert, 2000). COSMO-RS combines quantum chemical calculations (i.e, based on density functional theory) with statistical thermodynamics of molecular surface segments to more accurately predict thermodynamic properties such as chemical potentials, related activity coefficients, and solubility values. The solvent is treated like a continuum dielectric medium where the solute molecules are placed. The medium shields the solute's charge distribution, consequently affecting solvation energies and the interaction between the solvent and solute. The solvent S is considered as collection of pair-wise interacting segments, with the interaction energies between segment pairs defined based on the screening charge densities of σ and σ' of the corresponding sigma surfaces. Detailed information regarding the statistical thermodynamics equations are given, for example, in the work by Klamt and Eckert (Klamt and Eckert, 2000). As for computational implementation of the model, excipient molecules were modeled based on simplified structures and the screening charge densities of APIs for COSMOtherm (version 2022.0.0, Dassault Systèmes GmbH, Leverkusen, Germany) calculations were generated by the Turbomole package, version 7.4, using the Becke-Perdew (BP) BP86 density functional (Perdew, 1986) with a triple-zeta valence polarized (TZVP) TZVP34 basis set (BP-TZVP-COSMO template as implemented in COSMOconf by considering different conformers).

The screening charge densities of the polymers (i.e., so-called sigma profiles) were also built at a BP-TZVP-COSMO level theory. Following the COSMOtherm calculations of the chemical potentials, the software determined as the last step the activity coefficients, $\ln(\gamma_j)$ (equation 3):

$$\ln\left(\gamma_j\right) = \frac{\left(\mu_j^{(p)} - \mu_j^{(i)}\right)}{RT} \quad (3)$$

Where, $\mu_j^{(P)}$ is the chemical potential of the pure drug and $\mu_j^{(i)}$ is the respective chemical potential of the component j in the excipient matrix.

Activity coefficients of the different binary ASDs in the present work were calculated at two humidities 30 % RH and 75 % RH. For that purpose, calculations were performed on ternary systems, adding water, with water fraction values shown in Table S2.

To build the different polymer models, COSMOconf calculations were first performed on trimers of the different oligomeric unit constituting the polymer. The different trimers were later merged into one .mcos file representative of the polymer, where weight fractions of the different oligomers were assigned based on polymer chemical formula.

3. Results and discussion

3.1. Onset of instability

In the current study a combined in vitro in silico approach was investigated as a method to screen ASDs in early development, where the first step was to determine an onset of instability. Therefore, physical stability of ASDs with three APIs in the presence of ten pharmaceutically relevant polymers was investigated over a three-months period. The polymer amount was varied from a 1:3 API:polymer ratio to a lower 1:2 ratio (both as w/w), to assess the impact of polymer type and content on the physical stability of the generated ASDs. Furthermore, two temperature and two humidity conditions were investigated, resulting in three investigated conditions, namely 40 °C/ 75 %RH, 50 °C/ 30 %RH, and 50 °C/ 75 %RH. The condition of 40 °C/ 75 %RH is often used as an accelerated stress condition according to ICH (Q1A) (Sanjay Bajaj et al., 2012). PLM was used to determine the onset of instability and the first time point at which birefringence of a sample was detected (for at least one of the three replicas) was defined as the instability onset time. It should be highlighted that birefringence can arise from several factors, but it primarily corresponds to crystallization and demixing of the API and polymer phases, which marks the beginning of physical instability. Therefore, the term 'onset of instability' was used in this work to refer to any type of effect that would destabilize the ASD system. Another

API	Griseofulvin						
Polymer	/						
Ratio	/						
Time	0D	2D	1W	3W	6W	9W	12W
40/75 (°C/% RH)	A	C	C	C	C	C	C
	A	C	C	C	C	C	C
	A	C	C	C	C	C	C
50/75 (°C/% RH)	A	C	C	C	C	C	C
	A	C	C	C	C	C	C
	A	C	C	C	C	C	C
50/30 (°C/% RH)	A	C	C	C	C	C	C
	A	C	C	C	C	C	C
	A	C	C	C	C	C	C

API	Griseofulvin						
Polymer	PVP K30						
Ratio	1:2						
Time	0D	2D	1W	3W	6W	9W	12W
40/75 (°C/% RH)	A	C	C	C	C	C	C
	A	C	C	C	C	C	C
	A	C	C	C	C	C	C
50/75 (°C/% RH)	A	C	C	C	C	C	C
	A	C	C	C	C	C	C
	A	C	C	C	C	C	C
50/30 (°C/% RH)	A	A	A	A	A	A	A
	A	A	A	A	A	A	A
	A	A	A	A	A	A	A

API	Griseofulvin						
Polymer	PVP K30						
Ratio	1:3						
Time	0D	2D	1W	3W	6W	9W	12W
40/75 (°C/% RH)	A	C	C	C	C	C	C
	A	C	C	C	C	C	C
	A	A	C	C	C	C	C
50/75 (°C/% RH)	A	C	C	C	C	C	C
	A	C	C	C	C	C	C
	A	C	C	C	C	C	C
50/30 (°C/% RH)	A	A	A	A	A	A	A
	A	A	A	A	A	A	A
	A	A	A	A	A	A	A

API	Nifedipine						
Polymer	/						
Ratio	/						
Time	0D	2D	1W	3W	6W	9W	12W
40/75 (°C/% RH)	A	C	C	C	C	C	C
	A	C	C	C	C	C	C
	A	C	C	C	C	C	C
50/75 (°C/% RH)	A	C	C	C	C	C	C
	A	C	C	C	C	C	C
	A	C	C	C	C	C	C
50/30 (°C/% RH)	A	C	C	C	C	C	C
	A	C	C	C	C	C	C
	A	C	C	C	C	C	C

API	Nifedipine						
Polymer	PVP K30						
Ratio	1:2						
Time	0D	2D	1W	3W	6W	9W	12W
40/75 (°C/% RH)	A	A	A	A	C	C	C
	A	A	A	A	C	C	C
	A	A	A	A	C	C	C
50/75 (°C/% RH)	A	A	A	A	A	A	C
	A	A	A	A	A	A	C
	A	A	A	A	A	A	A
50/30 (°C/% RH)	A	A	A	A	A	A	A
	A	A	A	A	A	A	A
	A	A	A	A	A	A	A

API	Nifedipine						
Polymer	PVP K30						
Ratio	1:3						
Time	0D	2D	1W	3W	6W	9W	12W
40/75 (°C/% RH)	A	A	A	A	A	A	C
	A	A	A	A	A	A	C
	A	A	A	A	A	A	C
50/75 (°C/% RH)	A	A	A	A	A	A	A
	A	A	A	A	A	A	A
	A	A	A	A	A	A	A
50/30 (°C/% RH)	A	A	A	A	A	A	A
	A	A	A	A	A	A	A
	A	A	A	A	A	A	A

API	Felodipine						
Polymer	/						
Ratio	/						
Time	0D	2D	1W	3W	6W	9W	12W
40/75 (°C/% RH)	A	A	A	C	C	C	C
	A	A	A	C	C	C	C
	A	A	A	C	C	C	C
50/75 (°C/% RH)	A	A	A	C	C	C	C
	A	A	A	C	C	C	C
	A	A	A	C	C	C	C
50/30 (°C/% RH)	A	A	A	C	C	C	C
	A	A	A	C	C	C	C
	A	A	A	C	C	C	C

API	Felodipine						
Polymer	PVP K30						
Ratio	1:2						
Time	0D	2D	1W	3W	6W	9W	12W
40/75 (°C/% RH)	A	A	A	A	A	A	A
	A	A	A	A	A	A	A
	A	A	A	A	A	A	A
50/75 (°C/% RH)	A	A	A	A	A	A	A
	A	A	A	A	A	A	A
	A	A	A	A	A	A	A
50/30 (°C/% RH)	A	A	A	A	A	A	A
	A	A	A	A	A	A	A
	A	A	A	A	A	A	A

API	Felodipine						
Polymer	PVP K30						
Ratio	1:3						
Time	0D	2D	1W	3W	6W	9W	12W
40/75 (°C/% RH)	A	A	A	A	A	A	A
	A	A	A	A	A	A	A
	A	A	A	A	A	A	A
50/75 (°C/% RH)	A	A	A	A	A	A	A
	A	A	A	A	A	A	A
	A	A	A	A	A	A	A
50/30 (°C/% RH)	A	A	A	A	A	A	A
	A	A	A	A	A	A	A
	A	A	A	A	A	A	A

Fig. 2. Example of physical form and potential instability (crystallisation/demixing coded as C and amorphous coded as A) over time plots (i.e, days coded as D and weeks given as W) for the pure drugs and in presence of PVP K30 at the studied ratios and stress conditions. Green (fully amorphous), orange (moderate polarized light microscopy (PLM) signal observed), red (high PLM signal observed). Time plots for the remining ASDs that showed instability can be found in the supplementary section.

important point was about the term 'onset' in the context of time. As previously mentioned, the onset time was defined as the first time point where birefringence was detectable. Realistically, for many of the investigated ASDs, the onset of instability fell somewhere in between two measuring time points. Table 2 summarizes the onset of instability for each of the studied systems. ASDs that did not show instability within the three-month study duration are not included in the table.

Furthermore, an example of instability versus time chart is shown in Fig. 2 for the neat APIs and in presence of PVP K30. Time charts for the remainder of the systems can be found in Fig. S1a, S1b and S1c in the supplementary information.

The purpose of these charts was firstly to categorize the ASD films into fully amorphous systems or unstable mixtures, where initiation of instability in terms of developing demixing and crystallization over time was based on increased birefringence. Secondly, it was aimed to compare the impact of polymer type and content on the physical stability of the investigated ASDs using PLM, which is known to be sensitive to detect traces of crystallinity. However, a further quantification of crystallinity or further later-stage physical analytics was considered beyond scope of the present work on early ASD screening. No birefringence was observed on the PLM images before storage, indicating that the tested ASDs were all fully amorphous at the time of casting. An example of PLM images taken over time is shown in Fig. 3.

As can be observed from Table 2, the onset of instability for amorphous felodipine, in the absence of polymer, was significantly later than for griseofulvin and nifedipine. This was likely because felodipine is a GFA class III compound and therefore a slow crystallizer compared to the other two investigated APIs (Alhalaweh et al., 2015, Baird et al., 2010). The slower crystallization behavior of felodipine also resulted in stable ASDs with no instability observed in the systems containing polymer. On the other hand, the onset of instability for griseofulvin and nifedipine was detected on day 2 for all studied conditions, in line with their faster crystallization profile as GFA I and II, respectively (Baird et al., 2010). For griseofulvin ASDs in the harshest condition, at 50 °C/75 %RH, seven out of the ten tested polymers showed instability within the twelve-week stability study. PVP K30, PVP VA 64, Soluplus and HPMC AS LG, all exhibited an onset of instability within the first 7 days of monitoring, at least in the case of the lower API:polymer ratio. HPMC AS MG showed an instability onset within the first month for the ASDs with lower polymer content and within two months for the ASDs with a higher polymer content, emphasizing that an increase in polymer quantity could provide a greater degree of stabilization and therefore it could delay the onset of instability for those systems. On the other hand, for HPMC AS HG ASDs, the onset of instability was observed within the first month for the studied ratios. This agrees with the common understanding that lower polymer to drug ratios in ASDs represent more

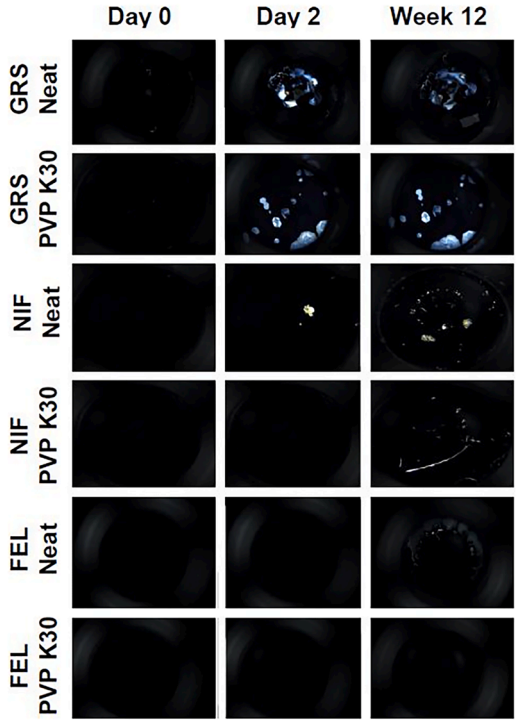

Fig. 3. Example of PLM images taken over time for the neat drugs and in presence of PVP K30. Griseofulvin (GRS), nifedipine (NIF) and felodipine (FEL).

challenging systems to stabilize physically (Liu et al., 2017, Newman and Zografi, 2023). Finally, HPMC E5 showed crystallization during the last month of storage. For the storage condition, at 40 °C/ 75 %RH, the behavior was like the one observed at 50 °C/ 75 %RH for the more hydrophilic polymers, PVP K30 and PVP VA 64. For the HPMC based systems, the onset of instability came later in time compared to the previous storage condition. For example, for HPMC AS LG, the onset time was observed in the middle of the second month at 40 °C/ 75 %RH, while it was observed on day 7 at 50 °C/ 75 %RH, when a 1:2 (w/w) API: polymer ratio was used and even later for the ASDs presenting a higher content of polymer.

Finally, for HPMC E5, the onset of instability was observed on day 63. This was surprising considering a higher temperature generally results in increase molecular mobility within the ASD. However, an elevated temperature can also result in formation of microdomains within the polymer matrix. This, in turn, can enhance the local solubility of the API in the polymer, thereby reducing the thermodynamic driving force for crystallization. While this phenomenon was not experimentally evaluated in the present study, it offers a possible explanation as to why the onset of instability at 50 °C/ 75 %RH was delayed compared to the 40 °C/ 75 %RH condition. For the griseofulvin ASDs incubated at 50 °C/ 30 %RH, instability was observed only in the presence of Soluplus, at day 42 for the lower polymer-content systems and at day 84 for the higher polymer-content ASDs. No instability was observed for any of the investigated Eudragit polymers at any of the tested conditions, suggesting that these polymers should be preferred for stabilizing of griseofulvin ASDs from a physical standpoint.

Nifedipine is a GFA class II compound and is therefore a slower crystallizer compared to griseofulvin (Alhalaweh et al., 2015, Baird et al., 2010). While the API itself showed instability already on day 2, in the presence of polymers, it was stable for most studied systems for the whole duration of the study. For this API, instability under the harshest storage conditions was observed for PVP K30, HPMC E5 and Eudragit L100 55. Virtually no difference was observed in the onset of instability time between the lower versus the higher-content polymer ASDs, but for ones containing PVP K30. Further, no instability was observed in the presence of Soluplus, Eudragit E100, or L100 as well as the HPMC AS polymers. Finally, at 50 °C/ 30 %RH all ASDs containing polymer were stable throughout the studied timeframe. As previously introduced, independently of the apparently simple binary system that composes an ASD, several parameters play into achieving satisfactory physical stability (Ricarte et al., 2019, Huang and Dai, 2014). Firstly, drug-polymer miscibility should be considered. If the two components are not homogenously blended, it can represent a first stage where the API separates into two amorphous phases from where crystallization would initiate from the drug-rich phase. The latter phase would have an unfavorably high drug-to-polymer ratio and a recent study on crystallization also demonstrated an accelerating crystallization for such phase-separating ASDs (Wolbert et al., 2022). In our study, the absence of birefringence at time zero indicated that the casted ASDs appeared macroscopically homogeneous without residual instability arising from sample preparation. However, it is important to specify that this does not rule out the possibility of amorphous phase separation, as such phenomena are not always detectable by birefringence alone. A second well known critical stability parameter is the glass transition temperature of the system. If polymeric matrix is carefully selected, the glass transition temperature of the mixture can help reducing molecular mobility in the formulation, whereby especially the α-relaxation should be minimized (Xie and Taylor, 2017, Péter-Haraszti et al., 2024). Furthermore, storage conditions also have a fundamental impact, as both temperature and humidity can act as plasticizers favoring instability and crystallization (Kapourani et al., 2020). The estimated wet T_g of the investigated formulations at the selected storage conditions, is then providing a measure of the

Table 3
Estimated wet T_g (°C) of the investigated formulations at the selected storage conditions determined as described in sections 2.3 and 2.4.

API	Polymer	25 °C - 30% RH*		25 °C - 75% RH*	
		1:2 (w/w)	1:3 (w/w)	1:2 (w/w)	1:3 (w/w)
Griseofulvin	Eudragit E100	54.3	52.1	50.0	48.0
	Eudragit L100	127.6	134.0	77.7	78.0
	Eudragit L100 55	83.3	83.6	44.9	41.8
	HPMC AS HG	94.9	96.8	68.1	67.4
	HPMC AS LG	93.1	94.7	66.4	65.5
	HPMC AS MG	93.3	95.0	66.3	65.4
	HPMC E5	109.2	113.3	54.8	52.4
	PVP K30	73.2	72.1	-24.9	-34.1
	PVP VA 64	74.4	73.6	-5.1	-12.7
	Soluplus	65.1	63.3	28.4	23.9
Nifedipine	Eudragit E100	45.2	45.4	41.2	41.6
	Eudragit L100	110.7	120.8	65.6	68.9
	Eudragit L100 55	69.5	73.2	34.7	34.3
	HPMC AS HG	79.5	85.0	55.4	57.9
	HPMC AS LG	77.7	82.9	53.8	56.0
	HPMC AS MG	77.7	83.0	53.5	55.8
	HPMC E5	92.2	100.0	43.3	43.9
	PVP K30	57.8	60.3	-30.9	-38.1
	PVP VA 64	59.6	62.3	-12.3	-17.7
	Soluplus	52.5	53.9	19.2	17.2
Felodipine	Eudragit E100	45.2	45.4	41.2	41.6
	Eudragit L100	110.7	120.8	65.6	68.9
	Eudragit L100 55	69.5	73.2	34.7	34.3
	HPMC AS HG	79.5	85.0	55.4	57.9
	HPMC AS LG	77.7	82.9	53.8	56.0
	HPMC AS MG	77.7	83.0	53.5	55.8
	HPMC E5	92.2	100.0	43.3	43.9
	PVP K30	57.8	60.3	-30.9	-38.1
	PVP VA 64	59.6	62.3	-12.3	-17.7
	Soluplus	52.5	53.9	19.2	17.2

* Water uptake of the ASDs was estimated at 30 %RH and 75 %RH at 25 °C. Although the ASDs were incubated at 40 °C and 50 °C, it can be assumed that the water uptake behavior, from a ranking perspective, would not change relative to 25 °C.

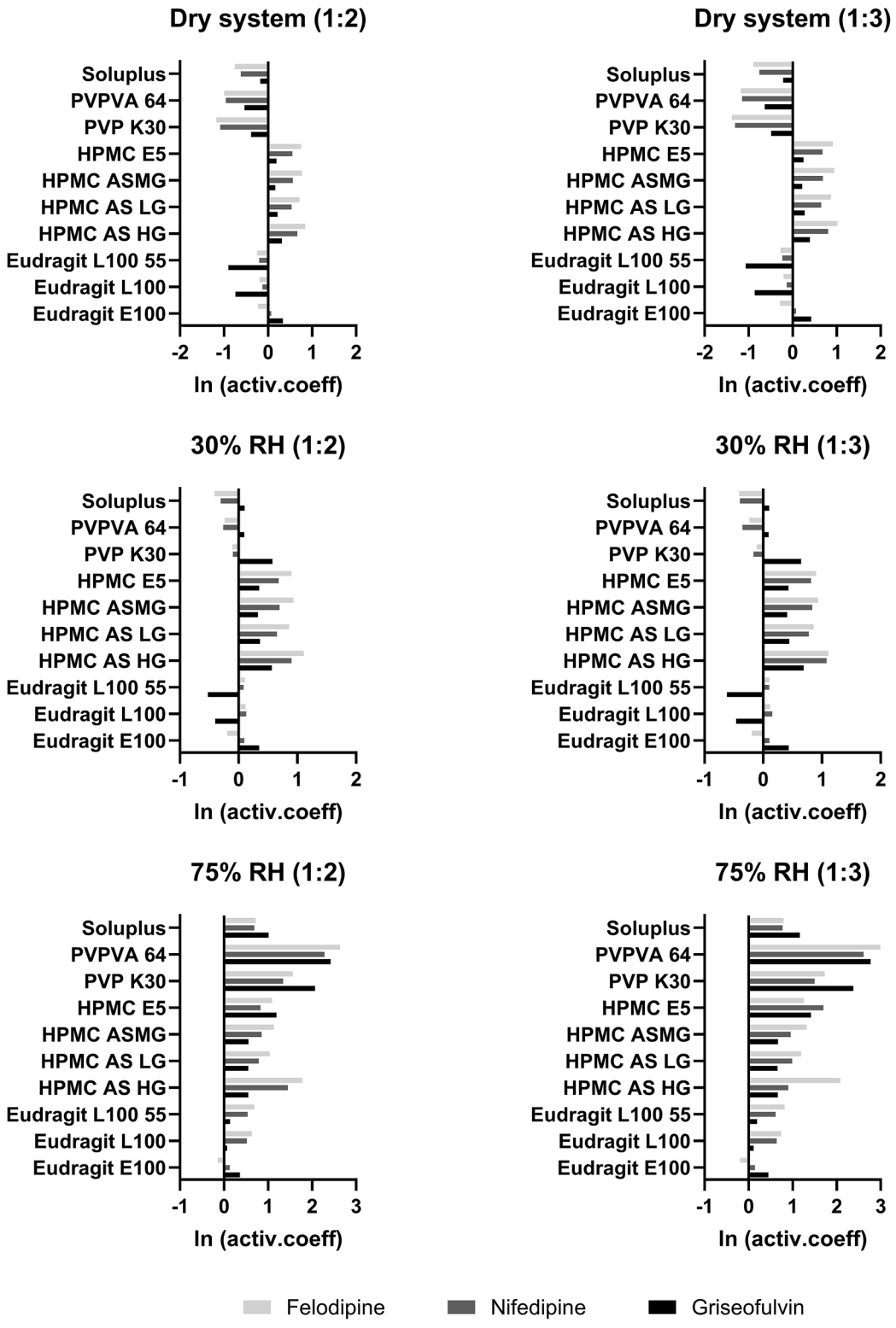

Fig. 4. Predicted interaction strength by means of the calculated activity coefficient between drug and polymer (active.coeff) for the wet and dry systems (details are given in the text).

molecular mobility domain of the ASDs, can be seen Table 3.

Considering the wet T_g of the ASDs containing griseofulvin, the more susceptible systems seemed to be those containing PVP K30, PVP VA 64 and Soluplus. This was expected based upon the hygroscopicity of these polymers and given that water has a strong plasticizing effect. The calculated wet T_g values reflected further the known different tendencies to absorb water, consequently providing different degrees of kinetic stabilization (Lehmkemper et al., 2018). Internal DVS measurements and manufacturer glass transition temperature values for the polymers studied can be found in Table S1 in the supplementary information. Soluplus was not as hygroscopic as the studied PVPs, however, it showed a relatively low T_g of 70 °C compared to that of 162 °C and 101 °C, of PVP K30 and PVP VA 64, respectively. In line with these observations, the ASDs containing these polymers were also the systems that

Table 4a
Observed alignment between the calculated interaction strength (activity coefficient) and physical stability (onset of instability in days) for griseofulvin-based ASDs. Highlighted in gray is the ASD that presented the weakest interaction strength but that was stable over the three-month study.

Griseofulvin							
1:2 (w/w) - API:Polymer				**1:3 (w/w) - API:Polymer**			
40°C/75%RH							
Polymer	ln (act. coeff)	Instability onset (days)	Expected? Y/N	Polymer	ln (act. coeff)	Instability onset (days)	Expected? Y/N
Eudragit L100 55	0.14	>84	Y	Eudragit L100 55	0.20	>84	Y
Eudragit E 100	0.37	>84	Y	Eudragit E 100	0.45	>84	Y
HPMC AS HG	0.56	>84	/	**HPMC AS LG**	**0.66**	**63**	**N**
HPMC AS LG	0.56	42	Y	HPMC AS HG	0.67	>84	Y
HPMC AS MG	0.56	21	Y	HPMC AS MG	0.67	>84	/
Soluplus	1.02	7	Y	Soluplus	1.17	7	Y
HPMC E5	1.20	2	Y	HPMC E5	1.42	2	Y
PVP K30	2.07	2	Y	PVP K30	2.38	2	Y
PVP VA 64	2.43	2	Y	PVP VA 64	2.78	7	Y
Neat API	/	2	/	Neat API	/	2	/
50°C/75%RH							
Eudragit L100	0.08	>84	Y	Eudragit L100	0.12	>84	Y
Eudragit L100 55	0.14	>84	Y	Eudragit L100 55	0.20	>84	Y
Eudragit E 100	0.37	>84	/	Eudragit E 100	0.45	>84	/
HPMC AS LG	0.56	7	Y	HPMC AS LG	0.66	21	Y
HPMC AS HG	0.56	21	Y	HPMC AS HG	0.67	21	Y
HPMC AS MG	0.56	21	Y	HPMC AS MG	0.67	42	Y
Soluplus	1.02	2	Y	Soluplus	1.17	2	Y
HPMC E5	1.20	63	Y	HPMC E5	1.42	84	Y
PVP K30	2.07	2	Y	PVP K30	2.38	2	Y
PVP VA 64	2.43	7	Y	PVP VA 64	2.78	2	Y
Neat API	/	2	/	Neat API	/	2	/
50°C/30%RH							
Eudragit L100	-0.53	>84	Y	Eudragit L100	-0.62	>84	Y
Eudragit L100 55	-0.41	>84	Y	Eudragit L100 55	-0.47	>84	Y
PVP VA 64	0.10	>84	Y	PVP VA 64	0.09	>84	Y
Soluplus	**0.11**	**42**	**N**	**Soluplus**	**0.10**	**84**	**N**
HPMC AS LG	0.34	>84	Y	HPMC AS LG	0.41	>84	Y
Eudragit E 100	0.35	>84	Y	HPMC AS MG	0.44	>84	Y
HPMC AS MG	0.35	>84	Y	Eudragit E 100	0.44	>84	Y
HPMC AS HG	0.37	>84	Y	HPMC AS HG	0.45	>84	Y
HPMC E5	0.57	>84	Y	PVP K30	0.65	>84	Y
PVP K30	0.58	>84	/	HPMC E5	0.70	>84	/
Neat API	/	2	/	Neat API	/	2	/

exhibited their instability onset the earliest, independently of the stress condition. Noteworthy is that this was not the case for nifedipine and felodipine. This could be explained by the slower tendency to crystallize of those APIs compared to griseofulvin (Panini et al., 2019, Alhalaweh et al., 2015, Mahlin and Bergstrom, 2013). On the other hand, HPMC AS polymers have a relatively high T_g of about 120 °C and a lower tendency towards water sorption (Butreddy, 2022, Borrmann et al., 2022). Hence, molecular mobility may not have been the leading cause of instability for these ASDs. Nevertheless, aside from HPMC AS HG, ASDs containing the MG and LG grades still showed instability in the higher humidity conditions. Supposing molecular mobility was not the driving force in this case, instability for these systems could be explained by the weak interaction (Fig. 4) between griseofulvin and the HPMC AS MG and LG polymers. All ASDs containing polymer placed at 50 °C/ 30 %RH, except the ones containing Soluplus, were stable. In the case of Soluplus this was explained by the lower T_g of this polymer combined with the higher

Table 4b
Observed alignment between the calculated interaction strength (activity coefficient) and physical stability (onset of instability in days) for nifedipine-based ASD. Highlighted in gray is the ASD that presented the weakest interaction strength but that was stable over the three-month study.

Nifedipine							
1:2 (w/w) - API:Polymer				**1:3 (w/w) - API:Polymer**			
40°C/75%RH							
Polymer	ln (act. coeff)	Instability onset (days)	Expected? Y/N	Polymer	ln (act. coeff)	Instability onset (days)	Expected? Y/N
Eudragit L100	**0.13**	**84**	**N**	Eudragit E100	0.15	>84	Y
Eudragit L100 55	**0.14**	**63**	**N**	**Eudragit L100 55**	**0.62**	**63**	**N**
Eudragit E 100	0.54	>84	Y	Eudragit L100	0.64	>84	Y
Soluplus	0.69	>84	Y	Soluplus	0.78	>84	Y
HPMC AS HG	0.79	>84	Y	HPMC AS HG	0.91	>84	Y
HPMC AS MG	0.83	>84	Y	HPMC AS MG	0.96	>84	Y
HPMC AS LG	1.86	>84	Y	HPMC AS LG	0.99	>84	Y
PVP K30	**1.35**	**42**	**N**	**PVP K30**	**1.50**	**84**	**N**
HPMC E5	**1.46**	**63**	**N**	**HPMC E5**	**1.70**	**63**	**N**
PVP VA 64	2.29	>84	/	PVP VA 64	2.62	>84	/
Neat API	/	2	/	Neat API	/	2	/
50°C/75%RH							
Eudragit L100	0.13	>84	Y	Eudragit L100	0.15	>84	Y
Eudragit L100 55	**0.52**	**42**	**N**	**Eudragit L100 55**	**0.62**	**42**	**N**
Eudragit E 100	0.54	>84	Y	Eudragit E 100	0.64	>84	Y
Soluplus	0.69	>84	Y	Soluplus	0.78	>84	Y
HPMC AS HG	0.79	>84	Y	HPMC AS HG	0.91	>84	Y
HPMC AS MG	0.83	>84	Y	HPMC AS MG	0.96	>84	Y
HPMC AS LG	0.86	>84	Y	HPMC AS LG	0.99	>84	Y
PVP K30	**1.35**	**84**	**N**	PVP K30	1.50	>84	Y
HPMC E5	**1.46**	**84**	**N**	**HPMC E5**	**1.70**	**84**	**N**
PVP VA 64	2.29	>84	/	PVP VA 64	2.62	>84	/
Neat API	/	2	/	Neat API	/	2	/
50°C/30%RH							
Soluplus	-0.31	>84	Y	Soluplus	-0.40	>84	Y
PVP VA 64	-0.27	>84	Y	PVP VA 64	-0.36	>84	Y
PVP K30	-0.10	>84	Y	PVP K30	-0.18	>84	Y
Eudragit L100	0.09	>84	Y	Eudragit L100	0.11	>84	Y
Eudragit E 100	0.10	>84	Y	Eudragit E 100	0.11	>84	Y
Eudragit L100 55	0.13	>84	Y	Eudragit L100 55	0.16	>84	Y
HPMC AS HG	0.66	>84	Y	HPMC AS HG	0.78	>84	Y
HPMC AS MG	0.69	>84	Y	HPMC AS MG	0.82	>84	Y
HPMC AS LG	0.70	>84	Y	HPMC AS LG	0.84	>84	Y
HPMC E5	0.90	>84	/	HPMC E5	1.08	>84	/
Neat API	/	2	/	Neat API	/	2	/

hygroscopicity (Table S1). Furthermore, polymer content seemed to have a notable impact, particularly in the case of the HPMC AS polymers, where a higher polymer content delayed the onset of instability for the harshest condition. Like humidity, temperature can have a plasticizing effect and lead to higher molecular mobility in the system. However, temperature also often promoted better miscibility between API and polymer (Pisay et al., 2023). This explains why in the case of HPMC E5, the instability onset for the 50 °C/ 75 %RH was observed significantly later than at 40 °C/ 75 % RH. Being a GFA class II drug, nifedipine should intrinsically present a lower tendency to crystallize compared to griseofulvin, which as mentioned is a GFA I class compound (Baird et al., 2010, Alhalaweh et al., 2015). This was in overall agreement with the findings obtained in the present study, however, for nifedipine, in absence of a polymer, the onset of instability was on day 2

as for griseofulvin, which therefore has a limited prediction capability for ASDs as mixtures. Nevertheless, it should be noticed that the first measurement following time zero was on day 2 and the onset happened somewhere between days 0 and 2; presumably taking place first for griseofulvin and then followed by nifedipine (Baird et al., 2010, Alhalaweh et al., 2015). Similarly to griseofulvin, the onset in the nifedipine ASDs containing HPMC E5 was earlier at the 40 °C/ 75 %RH condition compared to that at 50 °C/75 %RH. This further supports the idea that the higher temperature may have promoted better miscibility of this polymer with the API, thereby delaying the instability onset (Pisay et al., 2023). Nifedipine ASDs that exhibited instability within the studied timeframe were those containing PVP K30, Eudragit L100 55 and HPMC E5 at 50 °C/75 %RH. As previously mentioned for PVP K30, instability was likely driven by the plasticizing effect of humidity. In the case of Eudragit L100 55, instability may be explained by the poor API/polymer interaction at the higher humidity as can be seen in Fig. 4. When comparing the dry system to the wet ASD there was a significant worsening of the affinity between API and polymer once water was present. These data corresponded to the finding of other studies, i.e. that the presence of water did not only have a plasticizing effect but can further disrupt some of the interactions between API and polymer resulting in an overall reduced affinity to the polymer with a negative effect on ASD physical stability (Xie and Taylor, 2017, Tian et al., 2016, Lin et al., 2018)

3.2. Comparison of calculated activity coefficients and experimental results

COSMO-RS theory was employed to calculate the activity coefficients of drug in the polymer matrix. Thus, values greater than unity indicate that the drug experiences unfavorable interactions with the excipient, whereas values smaller than unity suggest favorable interactions of drug and polymer by means of hydrogen bonding, Van der Waals, or dipole interactions. The activity coefficients of the dry systems (i.e., composed of API and polymer alone) and of the wet systems are shown in Fig. 4.

Apart from the previously mentioned factors of reducing molecular mobility and external parameters such as humidity, the strength of the interaction between API and polymer is a well-known main driver to form a stable ASD (Walden et al., 2021, Wyttenbach et al., 2013, Lehmkemper et al., 2017). There is an inverse relationship between activity coefficient and interaction strength. The lower the ln of the activity coefficient, the stronger the interaction between API and polymer, thus resulting in a lower thermodynamic driving force towards phase separation and hence increased physical stability. Accordingly, the experimental onset of instability for each ASD was related to the calculated activity coefficient to evaluate a possible relationship between these parameters to guide excipient selection for future compounds that need to be formulated as ASDs. Table 4a and 4b show the studied ASDs ranked in order of decreasing activity coefficient. Therefore, the ASDs at the top represent the strongest interaction between API and polymer, while the ones at the bottom, the weakest.

The ASD that presented the weakest interaction strength but still was stable over the three-month study was identified for each API:polymer ratio and stress condition, see grey markings in Table 4a and 4b. For instance, for griseofulvin ASDs stored at 40 °C/ 75 %RH, in a 1:2 ratio, this corresponds to the ASD comprising griseofulvin with HPMC AS HG. It should be noted that although the ASDs containing the different grades of HPMC AS had the same activity coefficient, and hence interaction strength, only the one with HPMC AS HG was stable throughout the study, which was selected as a “reference”. The better stability of the ASDs containing the HPMC AS HG polymer was likely explained by the higher viscosity of this grade and therefore decreased molecular mobility (Butreddy, 2022). Assuming that a stronger interaction of drug and polymer would align with ASD stability, one would expect that all ASDs presenting a lower activity coefficient than the reference should have remained stable over the studied timeframe too. By contrast, for values of the activity coefficient being higher than that of the reference ASD, this tendency of relatively weaker interactions aligns with experimental findings of poor physical stability. This expectation of alignment is shown in the third column of Table 4a and 4b for each API:polymer ratio and stress condition. Any deviations from expected outcomes are marked in bold. For instance, for griseofulvin ASDs stored at 40 °C/ 75 % RH, in a 1:3 (w/w) ratio, this corresponds to the ASD comprising of griseofulvin with HPMC AS LG, because despite of having a slightly lower activity coefficient than the reference, this ASD was unexpectedly unstable. This was different for felodipine, in that no instability was observed for this API in presence of polymer. According to this assessment approach, an overall alignment between computational parametric calculations and binary experimental results (i.e. stable vs. unstable) was observed for 87 % of the studied ASDs. These results are encouraging and emphasize the ability of COSMO-RS to adequately group ASDs based on their performance on physical stability. Hence, providing preliminary guidance on excipient selection for development of stable ASDs. Despite the comparatively large number of systems studied in this work, more drugs would be necessary for each GFA class to draw conclusions on a statistical level. For the small number of ASDs that deviated from the expected results based on COSMO-RS calculations, molecular mobility was likely the leading cause. One first outlier was the ASD comprising griseofulvin and HPMC AS LG stored at 40 °C/ 75 %RH in the 1:3 (w/w) API:polymer ratio. As can be seen from Table 4a, the strength of interaction for the HPMC AS polymers was essentially the same across the different grades, however, only ASDs composed by HPMC AS LG were unstable, while no instability was observed for HPMC AS grade MG and HG. This is explained by the viscosity of these polymers. The LG grade has lowest viscosity amongst the three and, therefore, higher molecular mobility (Butreddy, 2022). On the other hand, surprisingly, ASDs containing any grade of HPMC AS polymer in a 1:2 (w/w) API:polymer ratio, were all stable. One aspect to be considered in this instance is that instability, including crystallization, is a stochastic process, which explains why instability was observed only in the ASDs composed of higher content of HPMC AS LG. For griseofulvin ASDs stored at 50 °C/ 30 %RH, it was observed that Soluplus deviated from what was expected by the activity coefficient calculations. For both API:polymer ratios, ASDs of griseofulvin with Soluplus, were unstable, despite exhibiting a stronger interaction with API compared to the reference ASD. This can be explained by a combination of molecular mobility and strength of interaction between API and polymer. When considering the wet T_g, presented in Table 3 and the stress temperature of 50 °C, molecular mobility was borderline between glassy and liquid domain. This can visually be seen in Fig. S2 in the supplementary section. In addition to molecular mobility, the interaction strength was here on a parametric scale compared to binary stability outcomes for simplicity, but this comes at the risk that for activity coefficients close to zero, there can be deviations from stability expectations. Nevertheless, a clear positive effect can be seen by the higher polymer content, where the onset of instability was only observed at the very end of the third month. In the case of nifedipine, for the 40 °C/ 75 % RH stress condition, PVP K30 HPMC E5 and Eudragit L100 55 were unstable, despite presenting better interaction strength compared to PVP VA 64. Also in this case, the explanation can be linked to the molecular mobility of these systems. Considering the humidity of 75 %RH, the ASD with PVP K30 falls in the deep liquid domain with a T_g of -30 and -38, for the 1:2 (w/w) and 1:3 (w/w) API:polymer ratios, respectively, fundamentally indicating less restricted motion of the molecules within those ASD. The ASD with HPMC E5 and Eudragit L100 55, instead, were borderline. With a T_g of 43 for the ASD containing HPMC E5 in a 1:2 (w/w) ratio and a T_g of 34.7 (1:2 w/w) and 34.3 (1:3 w/w) for the ASDs containing Eudragit L100 55, where molecules within the ASD start to exhibit more pronounced α-relaxation. The ASD comprising nifedipine and Eudragit E100 in a 1:2 (w/w) ratio exhibited instability on day 84. This was at the very end of the study and was not observed for

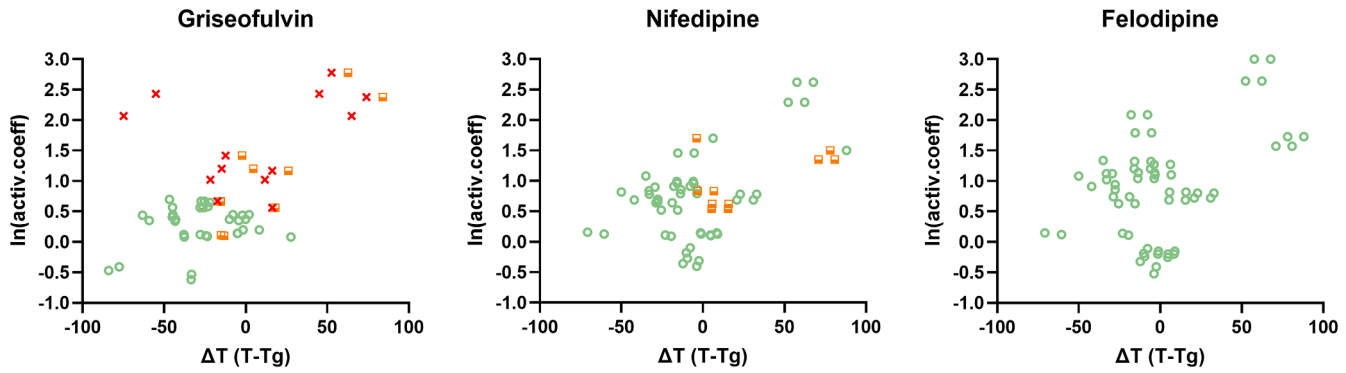

Fig. 5. Relationship between interaction strength and molecular mobility (as expressed by the temperature difference to T_g in°C) for the studied ASDs. Green dots: ASDs that did not exhibit instability over the studied timeframe. Orange squares: ASDs that exhibited instability within two months. Red crosses: ASDs that showed instability within one month.

any of the other studied ASDs, suggesting this was likely due to the stochastic nature of destabilizing processes such as crystallization. Another important observation was related to ASD containing PVP VA 64 at the higher humidity conditions. The estimated T_g for those systems were -12 °C and -17 °C for the 1:2 (w/w) and 1:3 (w/w) API:polymer ratios, respectively. This suggested that these ASDs would exhibit a comparatively high molecular α-relaxation. However, when looking at the interaction strength between nifedipine and PVP VA 64 for the dry system (see Fig. 4) it can be noticed that PVP VA 64 formed the strongest interaction compared to the other polymers. Finally, one should keep in mind that the estimated T_g values by the Gordon-Taylor equation can show notable deviations from true values, especially, in case of pronounced molecular interactions (Panini et al., 2019, Moustafine et al., 2006). Therefore, both the estimates of the mobility domain and water sorption were viewed as initial approximations in the framework of the screening approach presented. This resulted in an overestimation of the water sorption capacity of the system. The same reasoning can be applied to the ASDs comprising nifedipine in mixture with PVP K30, stored at 50 °C/ 75 %RH, where such a low T_g was resulting from an overestimation of the water sorption by the polymer.

3.3. Mapping interaction strength and molecular mobility domain regarding ASD physical stability

As discussed previously, different factors can influence the physical stability of an ASD, such as immiscibility between API and polymer, increased molecular mobility due to high temperature and/or humidity as well as the strength of interactions between API and polymer. Water, in particular, can significantly affect ASD stability. It competes with the API for binding to the polymer, increasing the thermodynamic driving force promoting crystallization (Wyttenbach et al., 2013, Xie and Taylor, 2017). Additionally, water has a plasticizing effect on molecular mobility, which further favors instability (Tian et al., 2016). Overall, the presence of water weakens interactions between the API and polymer, which can be reflected in a larger activity coefficient. These parameters were considered previously for a detailed comparison of solid dispersions that can be compared as being specific for a given drug, composition and storage condition, respectively (Table 4). To generally map molecular mobility domain and molecular interactions regarding physical stability, Fig. 5 shows the results for the different drugs.

In this analysis, the interaction strength (i.e. calculated activity coefficient) was plotted against the difference obtained by subtracting the T_g from the stress condition temperature. To evaluate the impact of these two parameters on ASD physical stability, the ASDs were divided into three categories depending on their instability onset time. The results for all stress conditions and API:polymer ratios were plotted together to have a more general view of the results. Fig. 5 can be visually divided into four virtual quadrants. In the upper right of the plots the ASDs that showed both high molecular mobility as well as weak interactions can be found. In the lower right quadrant are the systems located that have high molecular mobility but strong interactions. On the upper left are the systems that are in the glassy domain but that show poor interaction strength. Finally, the lower left quadrant contains the ASDs that showed, both, good interactions as well as being in the glassy domain. This way of plotting the data can provide visual guidance for selecting the most promising ASDs during early development. Generally, it may be possible to compute the interaction strength between API and polymer as well as estimate the T_g of the studied systems, finally generating a plot similar to the ones obtained in Fig. 5. Considering the ASDs without felodipine (for which no instability was obtained), selecting the ASDs in the lower left quadrant of the plot seemed a safe choice for obtaining physically stable ASDs. Although larger dataset of APIs would be required to corroborate current observations, the present pilot study provided consistent observations, despite of the different physico-chemical properties of the studied APIs as well as their different GFA classes. Finally, as previously explained, the water sorption of the PVP polymers was consistently overestimated. Therefore, the ASDs containing PVP were inaccurately positioned in the far upper right of the graphs in Fig. 5, clearly highlighted in Fig. S2 in the supplementary section, and would fall somewhere in the middle of the plot.

4. Conclusion

ASDs of three different APIs in the presence of ten pharmaceutically relevant polymers, at different ratios, were investigated for their physical stability under three accelerated stress conditions. The experimental results were compared to computational activity coefficient calculations obtained by COSMO-RS theory. The computational calculations were in alignment with a binary stability assessment and by considering the different ASDs relative to a reference, which yielded an overall success rate of 87 %. For the ASDs that deviated from the alignment with the computed activity coefficients, molecular mobility was likely the leading cause. While more experiments would be necessary to further confirm the proposed screening strategy, the present study provided insights and proposed an initial computational approach to aid excipient selection based on the activity coefficient obtained from COSMO-RS and wet T_g estimations. This strategy helps identifying formulations of physically stable ASDs by relying on computational and automated miniaturized experiments. Therefore, the presented in-vitro in-silico approach is promising for industrial stability screening of ASDs but would then have to be complemented with a separate biopharmaceutical screening approach for a viable industrial implementation.

CRediT authorship contribution statement

Egis Zeneli: Writing – review & editing, Writing – original draft,

Investigation, Formal analysis, Data curation, Conceptualization. **Hugo Bohets:** Writing – review & editing, Supervision, Methodology, Conceptualization. **Frédéric Ngono Mebenga:** Writing – review & editing, Methodology, Conceptualization. **René Holm:** Writing – review & editing. **Christophe Tistaert:** Writing – review & editing, Supervision, Conceptualization. **Martin Kuentz:** Writing – review & editing, Supervision, Funding acquisition, Writing – review & editing, Supervision, Conceptualization.

Declaration of competing interest

All authors report no conflicts of interest.

Acknowledgements

This project has received funding from the European Union's Horizon 2020 research and innovation program under the Marie Skłodowska-Curie grant agreement No. 955756.

Supplementary materials

Supplementary material associated with this article can be found, in the online version, at doi:10.1016/j.ejps.2025.107152.

Data availability

Data will be made available on request.

References

ALHALAWEH, A., ALZGHOUL, A., MAHLIN, D., BERGSTROM, C.A.S., 2015. Physical stability of drugs after storage above and below the glass transition temperature: relationship to glass-forming ability. Int. J. Pharm. 495, 312–317.
ANTOLOVIC, I., VRABEC, J., KLAJMON, M., 2024. COSMOPharm: drug-polymer compatibility of pharmaceutical amorphous solid dispersions from COSMO-SAC. Mol. Pharm. 21, 4395–4415.
ASGREEN, C., KNOPP, M.M., SKYTTE, J., LOBMANN, K., 2020. Influence of the polymer glass transition temperature and molecular weight on drug amorphization kinetics using ball milling. Pharmaceutics 12.
AULIFA, D.L., AL SHOFWAN, A.A., MEGANTARA, S., FAKIH, T.M., BUDIMAN, A., 2024. Elucidation of molecular interactions between drug-polymer in amorphous solid dispersion by a computational approach using molecular dynamics simulations. Adv. Appl. Bioinform. Chem. 17, 1–19.
BAIRD, J.A., TAYLOR, L.S., 2012. Evaluation of amorphous solid dispersion properties using thermal analysis techniques. Adv. Drug Deliv. Rev. 64, 396–421.
BAIRD, J.A., VAN EERDENBRUGH, B., TAYLOR, L.S., 2010. A classification system to assess the crystallization tendency of organic molecules from undercooled melts. J. Pharm. Sci. 99, 3787–3806.
BASF. 2022. *Kollidon VA 64* [Online]. Available: https://pharma.basf.com/products/kollidon-va-64 [Accessed 13.12.2023].
BASF. 2024. *Soluplus Technical Information* [Online]. Available: https://pharma.basf.com/products/soluplus [Accessed 13.12.2023].
BORRMANN, D., DANZER, A., SADOWSKI, G., 2022. Water sorption in glassy polyvinylpyrrolidone-based polymers. Membranes 12.
BUTREDDY, A., 2022. Hydroxypropyl methylcellulose acetate succinate as an exceptional polymer for amorphous solid dispersion formulations: A review from bench to clinic. Euro. J. Pharm. Biopharm. 177, 289–307.
DIEDENHOFEN, M., KLAMT, A., 2010. COSMO-RS as a tool for property prediction of IL mixtures—A review. Fluid Phase Equilib. 294, 31–38.
DUKECK, R., SIEGER, P., KARMWAR, P., 2013. Investigation and correlation of physical stability, dissolution behaviour and interaction parameter of amorphous solid dispersions of telmisartan: a drug development perspective. Eur. J. Pharm. Sci. 49, 723–731.
HIEW, T.N., ZEMLYANOV, D.Y., TAYLOR, L.S., 2022. Balancing solid-State stability and dissolution performance of lumefantrine amorphous solid dispersions: the role of polymer choice and drug-polymer interactions. Mol. Pharm. 19, 392–413.
HONARY, S., ORAFAI, H., 2002. The effect of different plasticizer molecular weights and concentrations on mechanical and thermomechanical properties of free films. Drug Dev. Ind. Pharm. 28, 711–715.
HUANG, Y., DAI, W.G., 2014. Fundamental aspects of solid dispersion technology for poorly soluble drugs. Acta Pharm. Sin. B 4, 18–25.
ILEVBARE, G.A., TAYLOR, L.S., 2013. Liquid–Liquid phase separation in highly supersaturated aqueous solutions of poorly water-soluble drugs: implications for solubility enhancing formulations. Cryst. Growth Des. 13, 1497–1509.
KAPOURANI, A., VARDAKA, E., KATOPODIS, K., KACHRIMANIS, K., BARMPALEXIS, P., 2020. Crystallization tendency of APIs possessing different thermal and glass related properties in amorphous solid dispersions. Int. J. Pharm. 579, 119149.
KLAMT, A., 2011. The COSMO and COSMO-RS solvation models. WIREs Computat. Molecul. Sci. 1, 699–709.
KLAMT, A., ECKERT, F., 2000. COSMO-RS: a novel and efficient method for the a priori prediction of thermophysical data of liquids. Fluid. Phase Equilib. 172, 43–72.
KOTHARI, K., RAGOONANAN, V., SURYANARAYANAN, R., 2014. Influence of molecular mobility on the physical stability of amorphous pharmaceuticals in the supercooled and glassy States. Mol. Pharm. 11, 3048–3055.
KUENTZ, M., HOLM, R., KRONSEDER, C., SAAL, C., GRIFFIN, B.T., 2021. Rational selection of bio-enabling oral drug formulations - A PEARRL commentary. J. Pharm. Sci. 110, 1921–1930.
LEHMKEMPER, K., KYEREMATENG, S.O., BARTELS, M., DEGENHARDT, M., SADOWSKI, G., 2018. Physical stability of API/polymer-blend amorphous solid dispersions. Eur. J. Pharm. Biopharm. 124, 147–157.
LEHMKEMPER, K., KYEREMATENG, S.O., HEINZERLING, O., DEGENHARDT, M., SADOWSKI, G., 2017. Impact of polymer type and relative humidity on the long-term physical stability of amorphous solid dispersions. Mol. Pharm. 14, 4374–4386.
LI, J., ZHAO, J., TAO, L., WANG, J., WAKNIS, V., PAN, D., HUBERT, M., RAGHAVAN, K., PATEL, J., 2015. The effect of polymeric excipients on the physical properties and performance of amorphous dispersions: part I, free volume and glass transition. Pharm. Res. 32, 500–515.
LIN, X., HU, Y., LIU, L., SU, L., LI, N., YU, J., TANG, B., YANG, Z., 2018. Physical stability of amorphous solid dispersions: a physicochemical perspective with thermodynamic. Kinetic Environ. Aspects. *Pharm Res* 35, 125.
LIU, X., FENG, X., WILLIAMS, R.O., ZHANG, F., 2017. Characterization of amorphous solid dispersions. J. Pharm. Investig. 48, 19–41.
LOSCHEN, C., KLAMT, A., 2015. Solubility prediction, solvate and cocrystal screening as tools for rational crystal engineering. J. Pharm. Pharmacol. 67, 803–811.
MAHLIN, D., BERGSTROM, C.A., 2013. Early drug development predictions of glass-forming ability and physical stability of drugs. Eur. J. Pharm. Sci. 49, 323–332.
MOUSTAFINE, R.I., ZAHAROV, I.M., KEMENOVA, V.A., 2006. Physicochemical characterization and drug release properties of eudragit E PO/eudragit L 100-55 interpolyelectrolyte complexes. Eur. J. Pharm. Biopharm. 63, 26–36.
NEWMAN, A., ZOGRAFI, G., 2023. Considerations in the development of physically stable high drug load API- polymer amorphous solid dispersions in the glassy State. J. Pharm. Sci. 112, 8–18.
PANINI, P., RAMPAZZO, M., SINGH, A., VANHOUTTE, F., VAN DEN MOOTER, G., 2019. Myth or truth: the glass forming ability class III drugs will always form single-phase homogenous amorphous solid dispersion formulations. Pharmaceutics 11.
PATRA, C.N., PRIYA, R., SWAIN, S., KUMAR JENA, G., PANIGRAHI, K.C., GHOSE, D., 2017. Pharmaceutical significance of Eudragit: A review. Futur. J. Pharm. Sci. 3, 33–45.
PÉTER-HARASZTI, A., ZÁHONYI, P., FARKAS, A., CSONTOS, I., NAGY, Z.K., SZABÓ, E., DEN MOOTER, G.V., MAROSI, G., 2024. Thermal investigation of relaxations of interacting and non-interacting amorphous solid dispersions. J. Therm. Anal. Calorim. 149, 8067–8083.
PERDEW, J.P., 1986. Density-functional approximation for the correlation energy of the inhomogeneous electron gas. Phys Rev B Condens Matter 33, 8822–8824.
VAN HOOGEVEST, P., LIU, X., FAHR, A., 2011. Drug delivery strategies for poorly water-soluble drugs: the industrial perspective. Expert Opin. Drug Deliv. 8, 1481–1500.
PISAY, M., NAVTI, P.D., RAO, V., KOTESHWARA, K.B., MUTALIK, S., 2023. Investigation of drug-polymer miscibility and design of ternary solid dispersions for oral bioavailability enhancement by Hot Melt Extrusion. J. Drug Deliv. Sci. Technol. 90.
PRICE, D.J., NAIR, A., KUENTZ, M., DRESSMAN, J., SAAL, C., 2019. Calculation of drug-polymer mixing enthalpy as a new screening method of precipitation inhibitors for supersaturating pharmaceutical formulations. Eur. J. Pharm. Sci. 132, 142–156.
QUE, C., DEAC, A., ZEMLYANOV, D.Y., QI, Q., INDULKAR, A.S., GAO, Y., ZHANG, G.G. Z., TAYLOR, L.S., 2021. Impact of drug-polymer intermolecular interactions on dissolution performance of copovidone-based amorphous solid dispersions. Mol. Pharm. 18, 3496–3508.
RICARTE, R.G., VAN ZEE, N.J., LI, Z., JOHNSON, L.M., LODGE, T.P., HILLMYER, M.A., 2019. Recent advances in understanding the micro- and nanoscale phenomena of amorphous solid dispersions. Mol. Pharm. 16, 4089–4103.
RUMONDOR, A.C., STANFORD, L.A., TAYLOR, L.S., 2009. Effects of polymer type and storage relative humidity on the kinetics of felodipine crystallization from amorphous solid dispersions. Pharm. Res. 26, 2599–2606.
SANJAY, BAJAJ, DINESH, SINGLA, SAKHUJA, N., 2012. Stability testing of pharmaceutical products. J. Appl. Pharm. Sci.
TAYLOR, A.C.F.R.L.S., 2009. Effect of polymer hygroscopicity on the phase behavior of amorphous solid dispersions in the presence of moisture. Mol. Pharm.
TIAN, B., TANG, X., TAYLOR, L.S., 2016. Investigating the correlation between miscibility and physical stability of amorphous solid dispersions using fluorescence-based techniques. Mol. Pharm. 13, 3988–4000.
TAYLOR, L.S., ZHANG, G.Z., 2016. Physical chemistry of supersaturated solutions and implications for oral absorption. Adv. Drug Deliv. Rev. 101, 122–142.
TIAN, Y., JACOBS, E., JONES, D.S., MCCOY, C.P., WU, H., ANDREWS, G.P., 2020. The design and development of high drug loading amorphous solid dispersion for hot-melt extrusion platform. Int. J. Pharm. 586, 119545.
WALDEN, D.M., BUNDEY, Y., JAGARAPU, A., ANTONTSEV, V., CHAKRAVARTY, K., VARSHNEY, J., 2021. Molecular simulation and statistical learning methods toward predicting drug-polymer amorphous solid dispersion miscibility, stability, and formulation design. Molecules 26.
WOLBERT, F., FAHRIG, I.K., GOTTSCHALK, T., LUEBBERT, C., THOMMES, M., SADOWSKI, G., 2022. Factors influencing the crystallization-onset time of metastable ASDs. Pharmaceutics 14.

WYTTENBACH, N., ALSENZ, J., GRASSMANN, O., 2007. Miniaturized assay for solubility and residual solid screening (SORESOS) in early drug development. Pharm. Res. 24, 888–898.
WYTTENBACH, N., JANAS, C., SIAM, M., LAUER, M.E., JACOB, L., SCHEUBEL, E., PAGE, S., 2013. Miniaturized screening of polymers for amorphous drug stabilization (SPADS): rapid assessment of solid dispersion systems. Eur. J. Pharm. Biopharm. 84, 583–598.
XIANG, T.X., ANDERSON, B.D., 2013. Molecular dynamics simulation of amorphous indomethacin-poly(vinylpyrrolidone) glasses: solubility and hydrogen bonding interactions. J. Pharm. Sci. 102, 876–891.
XIE, T., TAYLOR, L.S., 2017. Effect of temperature and moisture on the physical stability of binary and ternary amorphous solid dispersions of Celecoxib. J. Pharm. Sci. 106, 100–110.
ZHANG, S., LEE, T.W.Y., CHOW, A.H.L., 2019. Thermodynamic and kinetic evaluation of the impact of polymer excipients on storage stability of amorphous itraconazole. Int. J. Pharm. 555, 394–403.